Available online at www.sciencedirect.com
ScienceDirect
Journal of Power Sources 174 (2007) 1156–1160
JOURNAL OF POWER SOURCES
www.elsevier.com/locate/jpowsour

Short communication

Oxygen, hydrogen, ethylene and CO_2 development in lithium-ion batteries

M. Holzapfel *, A. Würsig [1], W. Scheifele, J. Vetter, P. Novák

Paul Scherrer Institut, Electrochemistry Laboratory, CH-5232 Villigen PSI, Switzerland

Available online 30 June 2007

Abstract

Gas evolution has been examined for different types of battery-related electrode materials via *in situ* differential electrochemical mass spectrometry (DEMS). Besides standard graphite also a novel silicon-based negative electrode was examined and it was shown that the evolution of hydrogen and ethylene is considerably reduced on this material compared to graphite. Oxygen evolution was proven to happen on the oxidative reaction of a Li_2O_2 electrode, besides a certain oxidation of the electrolyte. The 4.5 V plateau upon the oxidation of $Li[Ni_{0.2}Li_{0.2}Mn_{0.6}]O_2$ was likewise proven to be linked to oxygen evolution. Also in this case electrolyte oxidation was shown to be a side reaction. Layered positive electrode materials $Li(Ni,Co,Al)O_2$ and $Li(Ni,Mn,Co)O_2$ were also examined. The influence of different parameters on the CO_2 evolution in lithium-ion batteries was shown up. The amount of CO_2 formation is increased by high temperatures and cell voltages, while the addition of vinylene carbonate (VC) decreases it. $Li(Ni,Mn,Co)O_2$ shows much less CO_2 evolution than $Li(Ni,Co,Al)O_2$.
© 2007 Published by Elsevier B.V.

Keywords: Lithium batteries; Rechargeable; Gas evolution; Oxygen evolution; DEMS

1. Introduction

Gas evolution during storage and use is a major failure mechanism of lithium-ion batteries. Gases formed in the hermetically sealed cells may lead to internal pressure build-up and cell bulging, de-lamination of the electrodes and de-contacting of active material and thus present a safety risk. Reductive decomposition of the electrolyte on the negative electrode may form gas, depending on the electrolyte and the type of carbon used. On positive electrodes and during prolonged storage, especially at elevated temperature and high cell voltage CO_2 is the main gaseous compound formed [1,2]. According to previous investigations, CO_2 is mainly formed at the positive electrode due to oxidation of the electrolyte [2,3].

With the differential electrochemical mass spectrometry (DEMS) technique it is possible to detect the different gaseous reaction products that are evolved during cycling. Hence, intensity changes in mass signals can be detected as a function of time and/or potential and, thus, can be correlated with current peaks in the cyclic voltammogram or plateaus on galvanostatic charging/discharging curves.

In this study the evolution of different gases, studied via DEMS, will be discussed on both standard negative and positive electrode materials. Besides, novel systems as silicon-based negative electrodes or oxygen evolving positive electrodes will be presented.

2. Experimental

The measurement system [4] (Fig. 1) is based on headspace analysis. The gaseous reaction products are pumped off continuously from the top of the electrochemical cell via a capillary into a quadrupole mass spectrometer where they are analyzed on-line. With this electrochemical cell it is possible to identify even very small quantities of gas. The cell is also equipped with a heating unit for measurements at elevated temperature.

The electrodes were prepared by blade-coating the oxide and graphite directly on the titanium body of the DEMS cell. For the positive electrodes a mixture of 86.2 wt.% active oxide material, 7.4 wt.% TIMREX® KS6 graphite (TIMCAL SA, Bodio, Switzerland), 1.4 wt.% Super P carbon black (TIMCAL SA, Bodio, Switzerland) and 5 wt.% poly(vinylidene difluoride) binder (SOLEF 6020, Solvay SA, Belgium) was used. Because of eventual reaction of the CO_2 with metallic lithium, in the case of the oxide electrodes a graphite counter electrode was used for

* Corresponding author. Present address: Süd-Chemie AG, Ostenriederstr. 15, D-85368 Moosburg, Germany.
E-mail address: michael.holzapfel@sud-chemie.com (M. Holzapfel).
[1] Present address: Fraunhofer Institute for Silicon Technology (ISIT), Fraunhoferstr. 1, D-25524 Itzehoe, Germany.

0378-7753/$ – see front matter © 2007 Published by Elsevier B.V.
doi:10.1016/j.jpowsour.2007.06.182

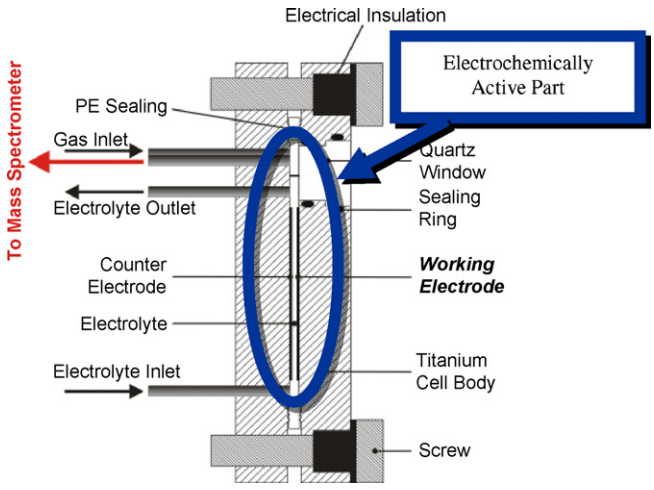

Fig. 1. Schematic drawing of the improved DEMS measurement cell for headspace gas analysis. For measurements at elevated temperature, heating plates can be attached to either side.

the measurements. The electrodes were balanced to be limited by the positive electrode active mass, with an excess of 30% on the graphite side, in order to avoid undesired side reactions at the negative electrode due to lithium plating. For graphite working or counter electrodes 95 wt.% active material were mixed with 5 wt.% poly(vinylidene difluoride) binder (SOLEF 6020, Solvay SA, Belgium). In both cases the slurries were prepared in *N*-methyl pyrrolidone (NMP). After the coating of the electrode material the cell parts were vacuum-dried at 120 °C over night. The measurements cell was assembled in an argon filled glove-box with a moisture and oxygen level of less than 5 ppm. During the measurements a constant stream of argon is flown through the headspace of the cell.

For the nano-silicon electrodes, 20% of silicon (Degussa AG, Marl, Germany) was added to the graphite and the electrodes were prepared as stated for graphite.

For the oxygen measurements on Li_2O_2 the experimental protocol is the following: ball-milled Li_2O_2 (Aldrich 90%), Super S carbon, electrolytical manganese dioxide (EMD) and PTFE (Aldrich) or Kynar 2810 (weight ratios: 16:80:2:2) are dispersed in NMP under argon and cast on the titanium cell body, the solvent evaporated and the electrodes dried at 120 °C over night. Approximately 55 mg of Li_2O_2 were used. Lithium was used as counter electrode. One mole of $LiPF_6$ in propylene carbonate (PC) was used as electrolyte.

For the measurements on $Li[Ni_{0.2}Li_{0.2}Mn_{0.6}]O_2$ a mixture of active material, Super S carbon and Kynar Flex 2801 binder in the weight ratios 80:10:10 in NMP was used, lithium as counter electrode and a 1 M solution of $LiPF_6$ in EC/DEC (1:2) as electrolyte.

For the oxide and graphite electrodes, the DEMS measurements were carried out potentiodynamically either at room temperature or 60 °C. A scan rate of 400 $\mu V\,s^{-1}$ was used for cyclic voltammetry (CV). For the nano-silicon electrodes the sweep rate was reduced to 100 $\mu V\,s^{-1}$. The CV measurements were started at open circuit potential (OCP). In the case of the graphite and silicon electrodes, the cell voltage was decreased from OCP to 5 mV in the first cycle, and then varied between 5 mV and 1.5 V. In the case of the oxide full cells, unless otherwise stated, the cell voltage was increased from OCP to 4.3 V in the first cycle, and then varied between 4.3 V and 3.0 V. For part of the measurements, a potentiostatic hold period was introduced both at the upper and lower voltage limit. For Li_2O_2 the cell potential was first stabilized at 4.2 V und then was raised in 100 mV steps every 120 min. For $Li[Ni_{0.2}Li_{0.2}Mn_{0.6}]O_2$ the cell potential was first stabilized at 4.3 V and then raised in 100 mV steps to 4.8 V every 120 min with a sweep rate of 0.1 $mV\,s^{-1}$.

The current and mass signals were recorded simultaneously both as a function of cell voltage and time.

Gases evolved at the electrode rise in the electrolyte to the headspace were they are pumped of, together with the argon carrier gas, via a capillary to the mass spectrometer. Mass signals were recorded on a Prisma QME 200 quadrupol mass spectrometer (Balzers AG/Pfeiffer Vaccuum). Electrochemical measurements were performed using standard laboratory test equipment (Astrol AG and Amel Instruments).

3. Results and discussion

3.1. Improvement of the cell design

The examination of gaseous reaction products coming from the reductive decomposition of organic carbonates on graphite upon the formation of the passivation film is relatively uncomplex due to the large amounts of gases formed. For this we used an old conventional DEMS cell design which is based on the diffusion of gases through a semi-permeable membrane situated below the active material. This cell is described in Ref. [5]. However if one passes to the reaction of positive electrode materials with electrolyte the amounts of gases are much smaller and the analysis cannot longer be done with the conventional cell. We, thus, designed a new cell based on headspace analysis of the gases. This cell is described in Section 2. In this cell the electrodes are in parallel and separated by 1 mm or less of electrolyte layer, whereas in the old cell the active material on the bottom and the lithium foil is immersed in the huge excess of electrolyte from above. Another advantage of the new cell design is that also different counter electrodes than lithium can easily be used. The main advantage of this cell, however, is the much higher amount of active material (50–300 mg) for the same amount of electrolyte (2.5 ml) in comparison to the old cell (10 mg for 2.5 ml). The difference in the detected signal is proportionally about 100 times higher for the new cell, as can be seen in Fig. 2 for the example of standard graphite (TIMREX® SFG6) in EC/DMC, 1 M $LiPF_6$. At potentials below 1 V versus Li/Li^+ ethylene evolution can be detected which arises from the reductive decomposition of EC on the graphite surface under formation of a passivating film.

With this new cell we then could examine the dependence of the CO_2 evolution upon the partial oxidation of electrolyte as a function of temperature type of material and possible additives.

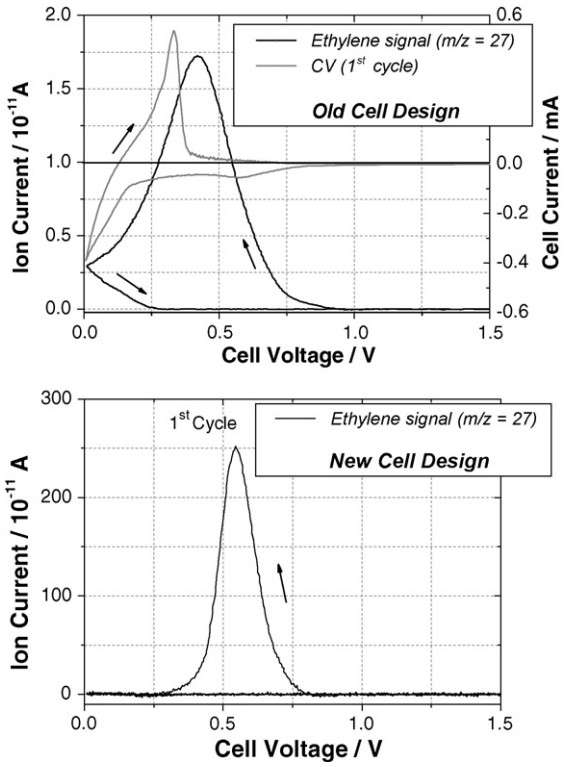

Fig. 2. Ethylene evolution in cells with TIMREX® SFG6 graphite in EC/DMC, 1 M $LiPF_6$ electrolyte at room temperature.

3.2. CO_2 evolution in layered oxide materials

3.2.1. Cell voltage and temperature

Investigations using $Li(Ni,Co,Al)O_2$ [6] as the positive active material showed a strong influence of the temperature on the onset voltage of CO_2 evolution (Fig. 3). The amount of CO_2 evolved is very low. For this reason for these experiments, 3% of Li_2CO_3 were added to the electrode to increase the amount of CO_2 evolved. It must be said also that CO_2 has a relatively high solubility in the electrolyte which does not facilitate its detection [7]. CO_2 evolution (in the first cycle) starts at a cell voltage of 4.9 V during the decrease of the voltage, and continues until a

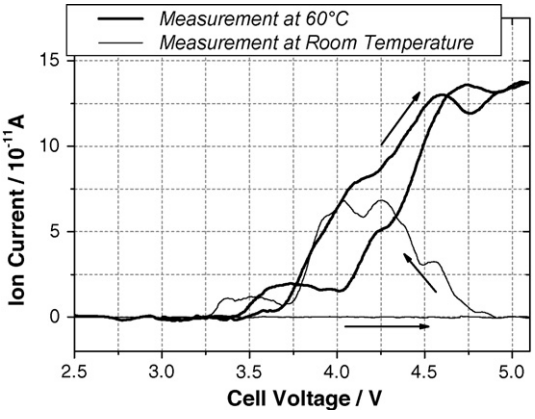

Fig. 3. CO_2 evolution in cells with $Li(Ni,Co,Al)O_2$ + 3% Li_2CO_3 cathodes at room temperature and at 60 °C.

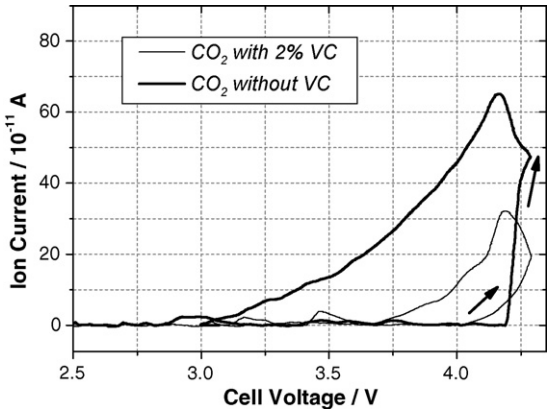

Fig. 4. CO_2 evolution in cells with $Li(Ni,Co,Al)O_2$ + 3% Li_2CO_3 cathodes at 60 °C, without VC and with 2% VC added to the electrolyte.

cell voltage of ca. 3.3 V is reached. At 60 °C the CO_2 evolution already starts at ca. 3.5 V during the increase of the voltage, continues until a cell voltage of 5.1 V is reached, and during the following discharge. From these results a decrease in the onset voltage for CO_2 evolution of ca. 1.4 V can be derived. As could have been expected, the overall amount of CO_2 generated is higher at elevated temperatures, indicated by higher ion currents in the MS.

3.2.2. Effect of vinylene carbonate

Vinylene carbonate (VC) is a well-known electrolyte additive for lithium-ion batteries, increasing the cycleability and reducing the irreversible capacity. In this study, we investigated the influence of VC on the CO_2 evolution of the cathode materials at elevated temperature. $Li(Ni,Co,Al)O_2$ with 3% of added Li_2CO_3 and the EC/PC/DMC, 1 M $LiPF_6$ electrolyte, with and without addition of 2% of vinylene carbonate was examined (Fig. 4). In the presence of VC, the onset voltage of CO_2 formation is slightly lower than in absence of the additive, but the total amount of CO_2 formed during the first cycle is smaller by a factor of around 3.

3.2.3. Lithium nickel manganese cobalt oxide

As a second positive active material, $Li(Ni,Mn,Co)O_2$ was tested on its CO_2 evolution in dependence of the cell voltage. It was found that a very small amount of CO_2 evolved from these electrodes at 60 °C which could only hardly be distinguished from the noise (Fig. 5). The material contains only very small amounts of Li_2CO_3, but addition of Li_2CO_3 gave somewhat contradictory results [6]. This is a strong hint that inorganic carbonate present in the $Li(Ni,Mn,Co)O_2$ has only a minor impact on the evolution of CO_2 at high voltages and elevated temperatures.

3.3. Oxygen evolution in $Li[Ni_{0.2}Li_{0.2}Mn_{0.6}]O_2$

Lithium may be extracted from lithium manganese-based oxides, such as Li_2MnO_3, containing Mn^{4+} ions, without oxidation of the transition metal ion. It was for a long-time not clear how this can be explained. H^+ ion exchange and simultaneous

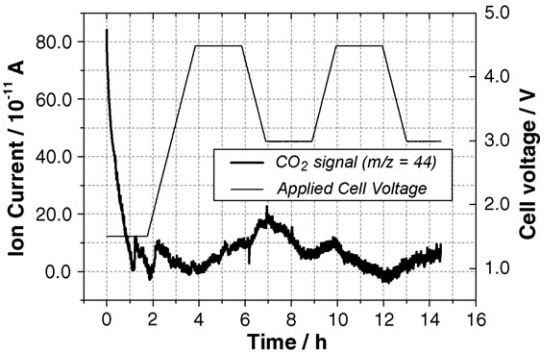

Fig. 5. CO_2 evolution in cells with Li(Ni,Mn,Co)O_2 cathodes and EC/PC/DMC, 1 M $LiPF_6$ electrolyte at 60 °C, with potentiostatic hold period at higher and lower voltage limit.

removal of Li and O has been proposed. In the latter case structural reorganisation of the material should occur (see [8] and references cited therein).

In $Li[Ni_xLi_{(1/3)-(2x/3)}Mn_{(2/3)-(x/3)}]O_2$ $(0 \le x \le 0.5)$, three Ni^{2+} ions substitute for two Li^+ ions and one Mn^{4+} ion in the layered compound Li_2MnO_3 ($Li[Li_{1/3}Mn_{2/3}]O_2$). This material shows short-range order of cations and can be described rather as a nanocomposite structure derived from a pseudo-binary $0.4LiNi_{0.5}Mn_{0.5}O_2{\cdot}0.6Li_2MnO_3$ system with $LiNi_{0.5}Mn_{0.5}O_2$ and Li_2MnO_3 end members. Following lithium deintercalation and the associated oxidation of Ni^{2+} to Ni^{4+}, lithium may continue to be extracted from this material despite the fact that all the manganese and nickel ions are in their fully charged (4+) oxidation state, and this with a high reversible capacity in excess of 200 mAh g^{-1}.

This process is associated with a well-defined plateau at 4.5 V, which corresponds then to the electrochemical removal of Li_2O (lithium extraction and oxygen loss) from the Li_2MnO_3 component of $xLiNi_{0.5}Mn_{0.5}O_2{\cdot}(1-x)Li_2MnO_3$ electrode structures, accompanied by oxygen loss and a condensation of manganese and nickel in the octahedral sites left vacant by the lithium ions.

Evolution of oxygen was observed with the DEMS technique. It became important from a potential of 4.6 V (Fig. 6), corresponding to the plateau at 4.5 V in the charge/discharge curve.

Table 1
Comparison of the different gases evolved upon electrochemical charging of $Li[Ni_{0.2}Li_{0.2}Mn_{0.6}]O_2$, Li_2O_2/EMD and Li_2O_2

m/z	Relative amounts of gas evolved for $Li[Ni_{0.2}Li_{0.2}Mn_{0.6}]_2$	Li_2O_2/EMD	Li_2O_2
12 (from CO and CO_2)	1.2	0.6	–
16 (from O_2, CO and CO_2)	15	7	0.3
28 (CO and CO_2)	14	12	1.6
32 (O_2)	100	100	1.1
44 (CO_2)	14	13	0.6

At the same time as oxygen also other gases were detected, as CO_2 and CO coming from partial oxidation of the electrolyte by the native oxygen. These gases could have been identified due to their secondary signals, e.g. CO_2 gives signals at $m/z = 44$ (CO_2), 28 (CO), 16 (O) and 12 (C), as shown in Table 1. These results provide direct evidence of oxygen evolution associated with the 4.5 V plateau.

3.4. Oxygen evolution in Li_2O_2

Oxygen cathodes have been employed in batteries that contain an aqueous electrolyte/air interface; the most well known is probably Zn/air. Their advantage compared to classic batteries is the low weight and thus high specific electrochemical capacity, as the oxygen is taken from and released into the air. In a system containing lithium ions in an organic electrolyte it was demonstrated that Li_2O_2 is the dominant discharge product [9] and recently it was shown that sustained charge/discharge cycling of Li_2O_2 is possible and that the Li_2O_2 formed on discharge, $2Li^+ + 2e^- + O_2 \rightarrow Li_2O_2$, is decomposed to $Li + O_2$ on charging when electrolytic manganese dioxide (EMD) is added as catalyst [10].

The decomposition of Li_2O_2 occurs also without EMD but the presence of the manganese oxide increases the amount of oxygen and lowers the potential and is therefore an active participant, aiding the charging process.

Direct evidence for O_2 evolution is given in Fig. 7 where, significant O_2 evolution was observed above 4.5 V in the case

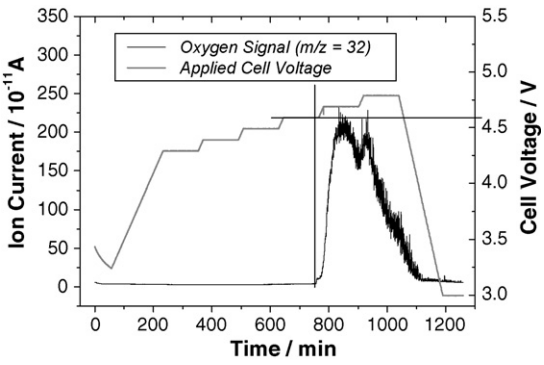

Fig. 6. Gas evolution vs. cell potential upon electrochemical charging of $Li[Ni_{0.2}Li_{0.2}Mn_{0.6}]O_2$.

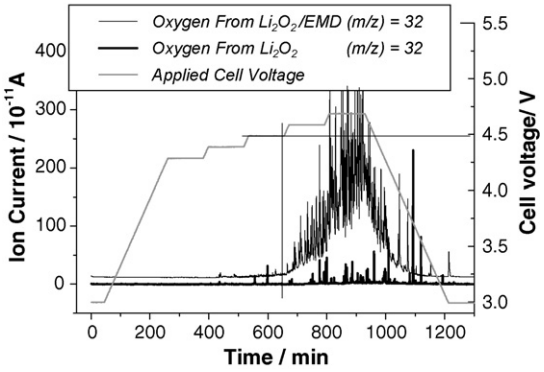

Fig. 7. Comparison of the oxygen evolution vs. cell potential upon electrochemical charging of Li_2O_2 and Li_2O_2/EMD.

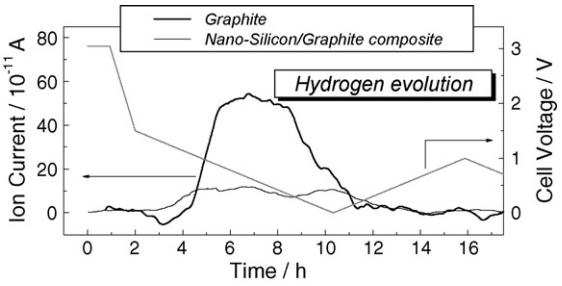

Fig. 8. Gas evolution for a nano-silicon graphite composite electrode compared to a graphite electrode upon the first electrochemical cycle (the hydrogen evolution is shown). The specific charge of both electrodes was comparable.

of the Li_2O_2/EMD. Li_2O_2 without EMD does show only a very low activity (and a cell without Li_2O_2 but with EMD gave no such oxygen evolution). Also in this case the amount of oxygen evolution far exceeded any other gases, the next most abundant being CO_2 and CO. The relative amounts of these gases, coming from the concomitant partial oxidation of the organic electrolyte by the oxygen are shown in Table 1.

3.5. Ethylene and hydrogen evolution at negative electrode materials, graphite and nano-silicon

Fig. 8 shows the comparative evolution of hydrogen for both nano-silicon and the graphite electrodes in the standard electrolyte EC:DMC (1:1), 1 M $LiPF_6$ + 2% VC. The active masses were calculated to have in both cases approximately the same total charge capacity per electrode. Thus the relative gas evolution can be compared directly. It can be seen that the gas evolution is four to five times less for the composite electrode which means that the nano-silicon does not significantly account for the reduction of the electrolyte under gas evolution (see also [11]). Graphite possesses a layered structure where the solvent molecules can partly be co-intercalated along with lithium ions, above all during the first cycle, when the passivation film which protects the graphite surface is not yet entirely formed. These solvent molecules are not stable at the low potential within the graphite upon further lithium intercalation, and are thus reduced under gas formation. Silicon does not present this layered structure, but a three-dimensional diamond-like structure. Solvent molecules can, hence, not be co-intercalated into the material but the only reaction occurs at the surface. It has been shown that a homogeneous passivation film is formed also on the surface of silicon; this passivation seems to protect the reduction of solvent relatively effectively, which reduces much the amount of gas formed.

For ethylene the amount of gas formed on the silicon electrode is also much reduced with respect to graphite (not shown here). The pressure build-up within a lithium-ion battery could thus be reduced, which increases the safety of the battery. A comparable result has already been described by Wagner et al. for tin-based electrodes [12].

4. Conclusions

A new cell system for *in situ* gas analysis via differential electrochemical mass spectrometry (DEMS) was developed. This cell shows a sensitivity which is increased by a factor of approximately 100 compared to the classical measurement system. Using this new cell it could be shown that in Li(Ni,Co,Al)O_2 positive electrode material and EC/PC/DMC, 1 M $LiPF_6$ electrolyte high temperatures promote the formation of CO_2. In the presence of vinylene carbonate in the electrolyte, the CO_2 evolution is reduced. Only very small amounts of CO_2 seem to be generated at Li(Ni,Mn,Co)O_2 at 60 °C. Nano-silicon-based negative electrode material shows a reduced gas (hydrogen, ethylene) evolution when compared to standard graphite. This is due to the fact that for the silicon the reduction of the electrolyte occurs only on the surface of the particles, as no co-intercalation of solvent is possible, due to the lacking two-dimensional structure.

$Li[Ni_{0.2}Li_{0.2}Mn_{0.6}]O_2$ and Li_2O_2, finally, were shown to develop oxygen upon positive polarization which goes along with some oxidation of the electrolyte as side reaction.

Acknowledgements

Financial support by the European Community and the Swiss State Secretariat for Education and Research under the framework of the European research project CAMELiA (ENK6-CT-2002-00636) is gratefully acknowledged. The groups of P.G. Bruce (University of St. Andrews, Scotland) and M.M. Thackeray (Argonne National Laboratory, USA) are gratefully acknowledged for their contributions to this work and M. Spahr (TIMCAL Ltd. Bodio, Switzerland) and F.-M. Petrat (Degussa AG, Marl, Germany) are acknowledged for the supply of the graphite and nano-silicon samples, respectively.

References

[1] K.H. Lee, E.H. Song, J.Y. Lee, B.H. Jung, H.S. Lim, J. Power Sources 132 (2004) 201.
[2] N. Takami, T. Ohsaki, H. Hasebe, M. Yamamoto, J. Electrochem. Soc. 149 (2002) A9.
[3] R. Imhof, P. Novák, J. Electrochem. Soc. 146 (1999) 1702.
[4] A. Würsig, J. Ufheil, P. Novák, Proceedings of the 205th ECS Meeting, no. 78, San Antonio, TX, USA, May 9–13, 2004.
[5] P. Novak, J.C. Panitz, F. Joho, M. Lanz, R. Imhof, M. Coluccia, J. Power Sources 90 (2000) 52.
[6] J. Vetter, M. Holzapfel, A. Würsig, W. Scheifele, J. Ufheil, P. Novák, J. Power Sources 159 (2006) 277.
[7] P. Kolar, H. Nakata, J.W. Shen, A. Tsuboi, H. Suzuki, A. Ue, Fluid Phase Equilibr. 228 (2005) 59.
[8] A.R. Armstrong, M. Holzapfel, P. Novak, C.S. Johnson, S.H. Kang, M.M. Thackeray, P.G. Bruce, J. Am. Chem. Soc. 128 (2006) 8694.
[9] K.M. Abraham, Z. Jiang, J. Electrochem. Soc. 143 (1996) 1.
[10] T. Ogasawara, A. Débart, M. Holzapfel, P. Novák, P.G. Bruce, J. Am. Chem. Soc. 128 (2006) 1390.
[11] M. Holzapfel, H. Buqa, L.J. Hardwick, M. Hahn, A. Würsig, W. Scheifele, P. Novák, R. Kötz, C. Veit, F.-M. Petrat, Electrochim. Acta 52 (2006) 973.
[12] M.R. Wagner, P.R. Raimann, A. Trifonova, K.C. Moeller, J.O. Besenhard, M. Winter, Electrochem. Solid State Lett. 7 (2004) A201.